Characterization of the interface adhesion of elastic-plastic thin film/rigid substrate systems using a pressurized blister test numerical model

Limei Jiang[a,b], Yichun Zhou[a*], Hongxiao Hao[a], Yanguo Liao[c], Chunsheng Lu[d]

[a] Key Laboratory of Low Dimensional Materials and Application Technology of Ministry of Education, Xiangtan University, Hunan 411105, China

[b] College of Packing & Printing, Hunan University of Technology, Hunan 412007, China

[c] Faculty of Mathematics and Physics, University of South China, Hunan 421001, China

[d] Department of Mechanical Engineering, Curtin University of Technology, Western Australia 6845, Australia

Abstract

The quality of interface adhesion of an elastic-plastic thin film/rigid substrate system can be characterized by its interface adhesion energy. To estimate the interface adhesion energy, a numerical model for the pressurized blister test has been proposed, which includes three steps: dimensional, forward and reverse analyses. The dimensional analysis is applied to derive a preliminary nondimensional relationship of the interface adhesion energy, and then the forward and reverse analyses are carried out to establish its explicit form and to extract the interface adhesion energy, respectively. The results are in good agreement with experimental measurements, which confirms the effectiveness of the model.

Keywords: Interface adhesion energy; Blister test; Elastic-plastic thin film; Dimensional analysis

[*] Corresponding author. Tel.: +86 731 58293586; fax: +86 731 58292468; E-mail address: zhouyc@xtu.edu.cn

1. Introduction

The elastic-plastic film/rigid substrate systems have been widely applied in microelectronic and magnetic recording industries and emerging technologies such as optical data transmission switches in a microelectromechanical system. Hence, the system failure caused by interface delamination or coating spallation attracts great attention. Previous studies have demonstrated that one of the most important intrinsic factors affecting the lifetime of a bi-material system is the quality of its interface adhesion. Therefore, the characterization of interface adhesion quality is an essential prerequisite in designing and optimizing the electrical and mechanical properties of a bi-material system (Scheu et al., 2006; Evans et al., 1999).

It is known that, in a linear elastic system, there are two commonly used quantities for the characterization of interface adhesion strength: one is the peak stress, $\hat{\sigma}$, at which interface debonding occurs under the uniaxial tension (Zhou et al., 2007; Morales-Rodríguez et al., 2007); and the other is the interface fracture toughness, Γ_{ss}, defined as the total fracture work per unit interfacial area at a steady state of crack growth (Gent and Lewandowski, 1987; Zhou and Hashida, 2003). The former is a direct indication of the adhesion strength between thin film and substrate that is widely accepted by materials scientists who mainly consider the applied loading as a key factor. Experts in mechanics think that, however, a coatings failure is dependent not only on the applied loading but also on flaws and defects located at the interface. Thus, they suggested that the interface fracture toughness, Γ_{ss}, which involves both the mechanical and geometrical factors, might characterize the quality of interface adhesion. In other words, the latter is more comprehensive than the former.

Although many experimental techniques have been developed over the past decades, the pressurized blister test is still one of the few methods that can deliver quantitative and meaningful

estimation on interfacial fracture toughness (Dannenberg, 1961), which has been applied to a variety of adhering systems. This testing method consists of applying pressure through a hole in the substrate to thin film bonded on it and causing delamination, as shown in Fig. 1. With help of a theoretical model, the interfacial fracture toughness can be evaluated from the height of the blister and the critical pressure applied during the growth of an interface crack.

In contrast to a linear elastic system where the interfacial fracture toughness is a constant and equal to the work of separation per unit area Γ_0 under the plane strain condition, it is hard to evaluate the interfacial fracture toughness in an elastic-plastic system. Owing to plastic dissipation, the energy dissipation Γ_{ss} during interface debonding is no longer equal to Γ_0. It is however the sum of two quantities, i.e., $\Gamma_{ss} = \Gamma_0 + \Gamma_p$, where Γ_0 is the energy consumed by interface separation in the fracture process zone and Γ_p is the energy dissipated by inelastic deformation in film and substrate. As plastic dissipation changes with the crack growth and geometrical properties of layers, Γ_{ss} is not a constant. Thus, it is inappropriate to use Γ_{ss} for characterizing the quality of interface adhesion of an elastic-plastic system.

The interface adhesion energy, Γ_0, being referred to the intrinsic interface property (Liu, 2001), is independent of the layer geometry and plastic dissipation in layers, which directly reflects the interface adhesion strength. As shown in our recent work (Jiang et al., 2008), the interface adhesion energy, Γ_0, can be used to characterize the quality of interface adhesion of an elastic-plastic film/rigid substrate system. Because of the nonlinear properties of elastic-plastic systems, it is difficult and even impossible to calculate the Γ_0 value. It is not surprising that, therefore, there is an unavailable formula that can be used in the blister test of elastic-plastic film bonded to rigid substrate. The finite element analysis, as done by Wei and Hutchinson (1997) for

the peeling test, could be alternative in this case. In their work (Wei and Hutchinson, 1997), some distinctions were made between Γ_0 and plastic dissipation in transient thin film peeling in terms of a traction-separation law, in which the primary parameters are Γ_0 and the peak traction, $\hat{\sigma}$. How to extract the traction-separation law (i.e., the determination of Γ_0 and $\hat{\sigma}$) has attracted many researchers' attention since several general traction-separation laws for damage-softened composites were obtained by slope measurements on double cantilever beam specimens (Ungsuwarungsri et al., 1987, 1988a, 1988b).

Swadener and Liechti (1988) proposed an iterative hybrid experimental/numerical approach, in which measurements and finite element predictions on the near-tip submicron crack opening displacement were matched to determine the traction separation law. Shirani and Liechti (1998) also used fracture process zone models, in which the traction-separation law for interface is calibrated in an iterative manner by comparing measurements with finite element predictions. First, the blister test is conducted in the volume control to determine the mechanical properties of thin film, pressure, volume and the crack opening displacement. Then, the finite element analysis that includes a traction-separation law for interface is performed. For an assumed traction-separation law (i.e., the known values of Γ_0 and $\hat{\sigma}$), the predicted values of critical pressure and central deflection can be obtained by finite element modeling. Finally, comparing these values with experimental measurements, the traction-separation law for the interface is calibrated in an iterative manner. During the iterative process, the number of iterations is dependent on the degree of closeness between the assumed traction-separation law and the practical one. If the assumed traction-separation law is close to the practical one, the number of iterations is few; otherwise a large number of iterations are needed.

Here, it is worth noting that, in the method of Shirani and Liechti (1998), there is a repeating process of debugging finite element analysis programs to make the assumed traction-separation law to approach the practical one. Hence, such a method is too complicated to be used in engineering applications. To overcome this difficulty, a numerical model is established to extract the interface adhesion energy of a bi-material system in the blister test, which includes three steps: dimensional, forward and reverse analyses. In comparison with previous research, the model can be easily used for characterization of the interface adhesion of an elastic-plastic thin film/rigid substrate system. It may also provide some clues on the establishment of empirical equations for evaluating Γ_0 of a dissimilar elastic-plastic material.

2. Numerical model

The thin film considered here is elastic-plastic and isotropic, and its constitutive relationship under the uniaxial tension is specified by

$$\varepsilon = \begin{cases} \sigma / E & \sigma \le \sigma_y \\ (\sigma_y / E)/(\sigma / \sigma_y)^{1/n} & \sigma > \sigma_y \end{cases} \tag{1}$$

where σ_y is the initial yield stress, n is the power hardening exponent, and E and v are Young's modulus and Poisson's ratio, respectively. To extract the interface adhesion energy of such a bi-material system with use of the blister test, a numerical method has been established which includes the following three steps:

Firstly, the dimensional analysis is applied to derive the relationship between the blister test and interface adhesion energy. Prior to the dimensional analysis, a comprehensive analysis of the blister test is necessary in order to scrutinize the factors that influence the critical pressure and their relative importance. Experiments (Dannenberg, 1961; Mougin et al., 2003) and numerical

analyses (Jiang et al., 2008; Guo et al., 2005; Hbaieb and Zhang, 2005) have revealed that the critical pressure P_c, at which separation is initiated, is a function of three dimensionless groups: the increment of crack advance Δa and layer geometry, interface adhesion, and material properties of film and substrate. For the sake of simplicity and neglecting unimportant parameters, the dimensional analysis is conducted to expose the essential relationship between these influencing parameters. The preliminary nondimensional function looks like

$$\frac{P_c}{\sigma_y} = f\left(\frac{\Gamma_0}{\sigma_y a}, \ldots\right) \tag{2}$$

where a is the radius of the central hole in substrate, as shown in Fig. 1.

Then, a forward analysis is carried out to establish the explicit form of Eq. (2). As displayed in Fig. 2, the forward analysis is comprised of two parts: (1) a geometrically nonlinear finite element analysis of the blister test of an elastic-plastic film bonded to a rigid substrate, and (2) the data fitting. Provided that the mechanical properties of film and substrate, layer geometry parameters, and interface adhesion parameters Γ_0 and $\hat{\sigma}$ are known, the critical pressure and central deflection can be obtained by finite element analysis. Generally, the initial yield stress σ_y and Young's modulus E for metals and alloys are about 30–1100 MPa and 40–210 GPa, respectively, and the hardening exponent n typically varies between 0.0 and 0.5 (Dao et al., 2001). Here, each set of these parameters (i.e., σ_y, E, v, n; t, a; Γ_0, $\hat{\sigma}$) is corresponding to a set of P_c and w_0. In order to gather enough data, a large amount of finite element simulations need to be carried out. These collected data will be used to establish the explicit nondimensional function of Eq. (2).

Finally, an effective reverse analysis algorithm is applied to extract the interface adhesion energy. The flow chart diagram of the reverse analysis algorithm is illustrated in Fig. 3. Here, the

elastic-plastic properties of the film are measured by the indentation test on a bi-material system (Liao et al., 2009), and the interface peak stress $\hat{\sigma}$ is measured by the uniaxial tensile test. With the help of a blister test, the critical pressure P_c, the critical central deflection w_0, and the amount of crack growth Δa can be obtained. Thus, the only remaining unknown parameter is the interface adhesion energy Γ_0, which is the focus of this paper. During the reverse analysis, the postulated interface adhesion energy may vary over a large range, and the extracted interface adhesion energy is one that makes the error of the explicit form of Eq. (2) be equal to or less than a specified infinitesimal constant e_0.

3. Finite element analysis

As mentioned, a geometrically nonlinear finite element analysis (FEA) is needed in the step two of the numerical model, which is conducted by using ABAQUS, a commercial general FEA package. Due to the symmetry, only half of the film and substrate is modeled, as shown in Fig. 4(a), in which a uniform pressure is applied to the de-bonded strip. The cohesive element in ABAQUS is used to characterize the interface properties of a dissimilar elastic-plastic material under the plane strain condition. Biased meshes are used in front of the initial crack tip to model the process of a crack growth. The smallest element size is denoted by Δ_0, as shown in Fig. 4(b). Due to the fact that the length quantity

$$R_0 = \frac{E\Gamma_0}{3\pi(1-\nu^2)\sigma_y^2} \tag{3}$$

scales with the size of plastic zone in the film, the ratio R_0/Δ_0 gives an indication of how well the mesh is able to resolve stress and strain fields around the crack tip. Based on the method proposed by Tvergaard and Hutchinson (1992), we have $R_0/\Delta_0 = 17.8$, which gives a reasonable

evaluation of the near-tip stress and strain fields and the fracture process zone.

The FEA to be carried out is similar to the numerical studies on the crack growth at an interface (Hbaieb and Zhang, 2005; Needleman, 1990; Shirani and Liechti, 1998; Tvergaard and Hutchinson, 1992, 1993). These numerical studies were based on an interface potential that specifies a traction-separation relationship being similar to the dependence of inter-atomic force on separation, as shown in Fig. 5. Here, a single non-dimensional separation measure λ is defined as

$$\lambda = \sqrt{\left(\frac{\delta_n}{\delta_n^c}\right)^2 + \left(\frac{\delta_t}{\delta_t^c}\right)^2} \tag{4}$$

where δ_n and δ_t denote the normal and tangential components of the relative displacement of crack faces across the interface in the fracture zone, and δ_n^c and δ_t^c are the critical values of displacement components. It is obvious that, when $\lambda = 1$, the traction drops to zero. As displayed in Fig. 5, the interface potential at which the traction is derived is defined as

$$\phi(\delta_n, \delta_t) = \delta_n^c \int_0^{\lambda} \sigma(\lambda')d\lambda' \tag{5}$$

The normal and tangential components of the traction acting on interface in the fracture process zone are given by

$$T_n = \frac{\partial \phi}{\partial \delta_n} = \frac{\sigma(\lambda)}{\lambda \delta_n^c}\delta_n \; ; \; T_t = \frac{\partial \phi}{\partial \delta_t} = \frac{\sigma(\lambda)}{\lambda}\frac{\delta_t \delta_n^t}{\delta_t^c \delta_t^c} \tag{6}$$

The traction law under a purely normal separation ($\delta_t = 0$) is $T_n = \sigma(\lambda)$, where $\lambda = \delta_n / \delta_n^c$, and under a purely tangential displacement ($\delta_n = 0$), $T_n = (\delta_n^c / \delta_t^c)\sigma(\lambda)$, where $\lambda = \delta_t / \delta_t^c$. The work of separation per unit area of interface can be obtained by Eq. (5) with $\lambda = 1$ and $\sigma(\lambda)$ illustrated in Fig. 5:

$$\Gamma_0 = \frac{\hat{\sigma}\delta_n^c(1-\lambda_1+\lambda_2)}{2} \tag{7}$$

In all these studies, the traction-separation law was implemented into an interface element through the UEL user subroutine in the finite element code ABAQUS. Recently, ABAQUS has developed a cohesive element although it does not include the trapezoidal traction-separation law. It has been found by Tvergaard and Hutchinson (1992, 1993) that the shape of the separation law is relatively unimportant. Thus, for the sake of simplicity, we set $\lambda_1 = \lambda_2$ in Eq. (7) and use a built-in cohesive element in ABAQUS as done in our early study (Jiang et al., 2008). Considering an essentially triangular traction-separation law, we have

$$\Gamma_0 = \frac{1}{2}\hat{\sigma}\delta_n^c \tag{8}$$

where Γ_0 and $\hat{\sigma}$ are the two most important parameters that characterize the fracture process in the model. Other features of the traction-separation law such as the relative peak of the shear traction to normal traction as specified by δ_n^c / δ_t^c, is taken to be unity (Shirani and Liechti, 1998).

4. Results and discussion

4.1. Elastic thin film/rigid substrate system

To verify the validity of the numerical model established above, an easy way is to compare the numerical result with the available analytical expression. According to the study done by Gent and Lewandowski (1987), we have the following formula on the critical pressure

$$P_c^4 = \frac{17.4Et\Gamma_0^3}{a^4} \tag{9}$$

and its dimensionless form can be rewritten as

$$\left(\frac{P_c}{E}\right)^4 = 17.4\left(\frac{t}{a}\right)\left(\frac{\Gamma_0}{aE}\right)^3 \tag{10}$$

The critical pressure P_c for the blister test of an elastic thin film/rigid substrate system is a function of three dimensionless groups: crack advance Δa and layer geometry, interface adhesion parameters, and film mechanical properties. The functional relationship can be written as

$$P_c = f(a, \Delta a, t, E, \nu, \hat{\sigma}, \Gamma_0) \tag{11}$$

where Poisson's ratio ν is not an important factor in the blister test, and for most engineering materials, $\nu \approx 0.3$ (Cheng and Cheng, 2004; Luo and Lin, 2007; Tunvisut et al., 2001). At the same time, the crack advance Δa was found to have the same effect as a. Furthermore, similar to the derivation of formula (9), the peak stress $\hat{\sigma}$ is fixed. Thus, ignoring the less important parameters, the following dimensionless form can be obtained

$$\frac{P_c}{E} = f\left(\frac{t}{a}, \frac{\Gamma_0}{aE}\right) \tag{12}$$

In comparison with Eq. (10), it is more convenient to choose $(P_c / E)^4$ as a dependent variable in the dimensionless function. So, Eq. (12) can be expressed as

$$\left(\frac{P_c}{E}\right)^4 = F\left(\frac{t}{a}, \frac{\Gamma_0}{aE}\right) \tag{13}$$

According to the numerical model, a forward analysis is then carried out to establish the explicit form of Eq. (13). As shown in Fig. 3, the forward analysis is composed of two parts: (1) a geometrically nonlinear FEA of the blister test of an elastic-plastic film bonded to a rigid substrate; and (2) the data fitting. In terms of the FEA and data fitting, the dependence of

$(P_c/E)^4$ on t/a and Γ_0/aE can be obtained, as shown in Fig. 6. It is obvious to see that, when t/a is fixed, the fitting function between $\left(\frac{P_c}{E}\right)^4$ and $\left(\frac{\Gamma_0}{aE}\right)$ can be assumed as

$$\left(\frac{P_c}{E}\right)^4 = \alpha\left(\frac{\Gamma_0}{aE}\right)^{\beta} \tag{14}$$

where α, β are the coefficient and exponent to be fitted, which are functions of t/a, that is, $\alpha(t/a)$ and $\beta(t/a)$. The values of α and β are listed in Table 1, where a different combination of α and β were obtained for each t/a. Plotting α versus t/a and β versus t/a and then fitting them, as shown in Figs. 7 and 8, we have

$$\alpha(t/a) = 17.3488(t/a) \tag{15}$$

$$\beta \approx 3.028 \tag{16}$$

Therefore, the explicit form of Eq. (14) can be established as

$$\left(\frac{P_c}{E}\right)^4 = 17.3488\left(\frac{t}{a}\right)\left(\frac{\Gamma_0}{aE}\right)^{3.028} \tag{17}$$

Obviously, it is well agreement with the analytical formula of Eq. (10). In other words, the numerical model can be used for extracting the interface adhesion energy of a bi-material system with the blister test.

4.2. Elastic-plastic thin film/rigid substrate system

Next, let us establish the dimensionless function of interface adhesion energy Γ_0 of an elastic-plastic thin film/rigid substrate system. The primary analysis revealed that the critical pressure P_c in the blister test of an elastic-plastic thin film/rigid substrate system is a function of the following parameters

$$P_c = P_c(a, \Delta a, t, \sigma_y, E, n, \nu, \hat{\sigma}, \Gamma_0) \tag{18}$$

As mentioned in Section 4.1, the influence of Δa and ν on the critical pressure P_c can be neglected. According to the dimensional analysis, the following dimensionless form can be obtained

$$\frac{P_c}{\sigma_y} = F\left[\frac{t}{a}, \frac{\sigma_y}{E}, n, \frac{\hat{\sigma}}{\sigma_y}, \frac{\Gamma_0}{\sigma_y a}\right] \tag{19}$$

Moreover, the FEA demonstrates that the initiation pressure is nearly a constant for different values of strain hardening exponents and the plastic zones at the level of pressure are similar, as shown in Figs. 9 and 10. These observations are consistent with that reported by Hbaieb and Zhang (2005). Hence, the strain hardening exponent n is assumed to be a constant of 0.2. In order to further reduce the number of parameters in Eq. (19), the ratio t/a is set to be several typical values such as, (1) $t/a = 0.0153$ with a = 3.25 mm and t =50 μm, (2) $t/a = 0.0062$ with a = 3.25 mm and t = 20 μm, and (3) $t/a = 0.0333$ with a = 1.5 mm and t = 50 μm. Then, we only need to establish the following dimensionless function for each typical value

$$\frac{P_c}{\sigma_y} = F\left(\frac{\sigma_y}{E}, \frac{\hat{\sigma}}{\sigma_y}, \frac{\Gamma_0}{\sigma_y a}\right) \tag{20}$$

Here, the dependence of $\frac{P_c}{\sigma_y}$ on the dimensionless parameters are also studied by using the FEA package ABAQUS. The parameter study revealed that the relationships between $\frac{P_c}{\sigma_y}$ and the parameters ($\frac{\sigma_y}{E}$, $\frac{\hat{\sigma}}{\sigma_y}$, $\frac{\Gamma_0}{\sigma_y a}$) are approximately linear, similar to those reported by Hbaieb and Zhang (2005). Therefore, a linear fitting function is chosen here. Finally, the following equation can be established by fitting the FEA results

$$\frac{P_c}{\sigma_y} = A_1 + A_2 \frac{\sigma_y}{E} + \left(A_3 + A_4 \frac{\sigma_y}{E} \right) \frac{\hat{\sigma}}{\sigma_y} + \left[B_1 + B_2 \frac{\sigma_y}{E} + \left(B_3 + B_4 \frac{\sigma_y}{E} \right) \frac{\hat{\sigma}}{\sigma_y} \right] \frac{\Gamma_0}{\sigma_y a} \tag{21}$$

where A_1, …, A_4 and B_1, …, B_4 are the coefficients to be fitted, as listed in Table 2. Once the explicit form of the dimensionless function is obtained, the interface adhesion energy Γ_0 of an elastic-plastic thin film/rigid substrate system can be extracted by the reverse analysis algorithm illustrated in Fig. 3.

4.3. Effectiveness of the reverse analysis

Using fracture process zone models, Shirani and Liechti (1998) obtained the adhesive adhesion energy of thin elastic-plastic thin films on rigid substrate from circular blister experiments. Table 3 lists the material properties and critical pressure determined by Shirani and Liechti (1998), together with the finally estimated interface adhesion energy. Here, a reverse analysis was done in order to extract the interface adhesion energy of the same material system. Following the reverse analysis illustrated in Fig. 3, the interface adhesion energy that minimizes the error of Eq. (21) can be calculated. The result is also listed in Table 3, which is very close to the interface adhesion energy extracted by Shirani and Liechti (1998). That is, the effectiveness of the reverse analysis has been clearly demonstrated.

5. Conclusions

In this paper, we extended our recent study on characterization of the quality of interface adhesion of an elastic-plastic materials system. A numerical model has been proposed to extract the interface adhesion energy of a bi-material system with the blister test, which includes three steps: firstly, the dimensional analysis is applied to derive a preliminary nondimensional

relationship between the blister test and the interface adhesion energy. Then, a forward analysis is carried out to establish the explicit form of this nondimensional relationship. Finally, a reverse analysis is performed to extract the interface adhesion energy. With the numerical model, we obtained the dimensionless functions of interface adhesion energy of elastic and elastic-plastic thin film/rigid substrate systems, which are in good agreement with the analytical formula and experimental results. Compared to previous studies, the characterization of interface adhesion of an elastic-plastic thin film/rigid substrate system in practical applications becomes much easier. This study also provides some guidelines on the establishment of an empirical equation for evaluating the interface adhesion energy of dissimilar elastic-plastic materials.

Acknowledgements

This work has been supported by the National Natural Science Foundation of China (Grant Nos. 50531060, 10525211 and 10828205) and the Cultivation Fund of the Key Scientific and Technical Innovation Project, the Ministry of Education of China (Grant No. 076044).

References

Cheng, Y.T., Cheng, C.M., 2004. Scaling, dimensional analysis, and indentation measurements. Mater. Sci. Eng. R 44, 91–149.

Dannenberg, H., 1961. Measurement of adhesion by a blister method. J. Appl. Polym. Sci. 5, 125–134.

Dao, M., Chollacoop, N., Van Vliet, K.J., Venkatesh, T.A., Suresh, S., 2001. Computational modeling of the forward and reverse problems in instrumented sharp indentation. Acta Mater. 49, 3899–3918.

Evans, A.G., Hutchinson, J.W., Wei, Y., 1999. Interface adhesion: effects of plasticity and segregation. Acta Mater. 47, 4093–4113.

Gent, A.N., Lewandowski, L.H., 1987. Blow-off pressures for adhering layers. J. Appl. Polym. Sci. 33, 1567–1577.

Guo, S., Wan, K.T., Dillard, D.A., 2005. A bending-to-stretching analysis of the blister test in the presence of tensile residual stress. Int. J. Solids Struct. 42, 2771–2784.

Hbaieb, K., Zhang, Y.W., 2005. A parametric study of a pressurized blister test for an elastic-plastic film-rigid substrate system. Mater. Sci. Eng. A 390, 385–392.

Jiang, L.M., Zhou, Y.C., Liao, Y.G., Sun, C.Q., 2008. A pressurized blister test model for the interface adhesion of dissimilar elastic-plastic materials. Mater. Sci. Eng. A 487, 228–234.

Liao, Y.G., Zhou, Y.C., Huang, Y.L., Jiang, L.M., 2009. Measuring elastic-plastic properties of thin films on elastic-plastic substrates by sharp indentation. Mech. Mater. 41, 308–318.

Liu, P., Cheng, L., Zhang, Y.W., 2001. Measuring interface parameters and toughness: a computational study. Acta Mater. 49, 817–825.

Luo, J., Lin, J., 2007. A study on the determination of plastic properties of metals by instrumented indentation using two sharp indenters. Int. J. Solids Struct. 44, 5803–5817.

Morales-Rodríguez, A., Moevus, M., Reynaud, P., Fantozzi, G., 2007. Strength enhancement of 2D-SiC_f/SiC composites after static fatigue at room temperature. J. Eur. Ceram. Soc. 27, 3301–3305.

Mougin, J., Dupeux, M., Antoni, L., Galerie, A., 2003. Adhesion of thermal oxide scales grown on ferritic stainless steels measured using the inverted blister test. Mater. Sci. Eng. A 359, 44–51.

Needleman, A., 1990. An analysis of decohesion along an imperfect interface. Int. J. Fract. 42, 21–40.

Scheu, C., Gao, M., Oh, S.H., Dehm, G., Klein, S., Tomsia, A.P., Rühle, M., 2006. Bonding at copper-alumina interfaces established by different surface treatments: a critical review. J. Mater. Sci. 41, 5161–5168.

Shirani, A., Liechti, K.M., 1998. A calibrated fracture process zone model for thin film blistering. Int. J. Fract. 93, 281–314.

Swadener, J.G., Liechti, K.M., 1988. Asymmetric shielding mechanisms in the mixed-mode fracture of a glass/epoxy interface. J. Appl. Mech. 65, 25–39.

Tvergaard, V., Hutchinson, J.W., 1992. The relation between crack growth resistance and fracture process parameters in elastic-plastic solids. J. Mech. Phys. Solids 40, 1377–1397.

Tvergaard, V., Hutchinson, J.W., 1993. The influence of plasticity on mixed mode interface toughness. J. Mech. Phys. Solids 40, 1119–1135.

Tunvisut, K., O'Dowd, N.P., Busso, E.P., 2001. Use of scaling functions to determine mechanical properties of thin coatings from microindentation tests. Int. J. Solids Struct. 38, 335–351.

Ungsuwarungsri, T., Knauss, W.G., 1987. The role of damage-softened material behavior in the fracture of composites and adhesives. Int. J. Fract. 35, 221–241.

Ungsuwarungsri, T., Knauss, W.G., 1988a. A nonlinear analysis of an equilibrium craze: Part I – problem formulation and solution. J. Appl. Mech. 55, 44–51.

Ungsuwarungsri, T., Knauss, W.G., 1988b. A nonlinear analysis of an equilibrium craze: Part II – simulations of craze and crack growth. J. Appl. Mech. 55, 52–58.

Wei, Y., Hutchinson, J.W., 1997. Nonlinear delamination mechanics for thin films. J. Mech. Phys. Solids 45, 1137–1159.

Zhou, H., Li, F., He, B., Wang, J., Sun, B.D., 2007. Air plasma sprayed thermal barrier coatings on titanium alloy substrates. Surf. Coat. Technol. 201, 7360–7367.

Zhou, Y.C., Hashida, T., 2003. Determination of interface fracture toughness in thermal barrier coating system by blister tests. J. Eng. Mater. Technol. 125, 176–182.

Figure captions

Fig. 1. Schematic representation of the pressurized blister test.

Fig. 2. The flow chart program for establishing the dimensionless function.

Fig. 3. The flow chart program for determining the interface adhesion energy Γ_0 by using the reverse analysis.

Fig. 4. The computational model for the blister test (a) and FEA mesh of the crack tip zone (b).

Fig. 5. Illustration of the traction separation law.

Fig. 6. The dimensionless parameter $\left(\frac{P_c}{E}\right)^4$ versus $\left(\frac{\Gamma_0}{aE}\right)$ for several values of t/a : (a) $t/a = 0.0154$; (b) $t/a = 0.0031$; (c) $t/a = 0.01$, (d) $t/a = 0.002$.

Fig. 7. Relationship between the coefficient α and t/a .

Fig. 8. Relationship between the exponent β and t/a .

Fig. 9. Dependence of pressure on the strain-hardening exponent.

Fig. 10. Plastic zones of thin film near the crack tip for several values of the strain-hardening exponent: (a) n = 0.2; (b) n = 0.3; and (c) n = 0.4. The region from light blue to red represents the equivalent plastic strain that is more than zero, in which blue and red colors correspond to the minimum and maximum equivalent plastic strains, respectively.

Table 1. The fitted coefficient α and exponent β by using Eq. (14) to the FEA results with various values of *t*/*a*.

t/*a*	α	β
0.0154	0.2528	3.0256
0.0031	0.0554	3.0397
0.01	0.1447	2.9991
0.002	0.0305	3.0222

Table 2. The coefficients by fitting Eq. (21) to the FEA results.

Coefficient	$t/a = 0.0154$	$t/a = 6.1538\times10^{-3}$	$t/a = 0.0333$
A_1	0.0134	5.2687×10^{-3}	-1.9640×10^{-2}
A_2	−4.7476	−1.9878	9.7041
A_3	-5.1091×10^{-4}	-1.2145×10^{-4}	1.3605×10^{-2}
A_4	0.7946	0.5186	−4.9997
B_1	7.5980×10^{2}	-7.0102×10^{3}	1.7993×10^{4}
B_2	1.3911×10^{6}	5.1004×10^{6}	-6.7784×10^{6}
B_3	-3.0221×10^{3}	1.8511×10^{3}	8.6346×10^{3}
B_4	-1.0984×10^{5}	4.5406×10^{5}	-2.5767×10^{6}

Table 3. The comparison of experimental data from Shirani and Liechti (1998) and Γ_0 obtained by the reverse analysis.

t/a	E (GPa)	σ_y (MPa)	$\hat{\sigma}$ (MPa)	P_c (MPa)	Γ_0 (N/m)	
					Experimental (Shirani and Liechti, 1998)	Reverse analysis
0.0154	2.15	31	140	0.78	390	410.81

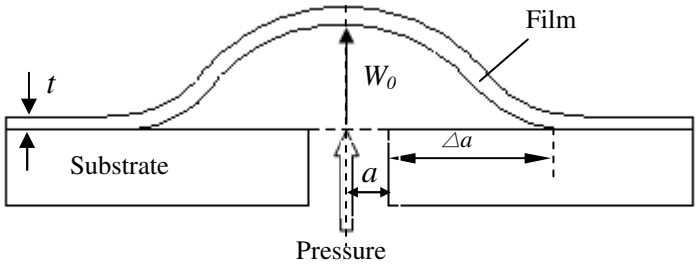

Fig. 1

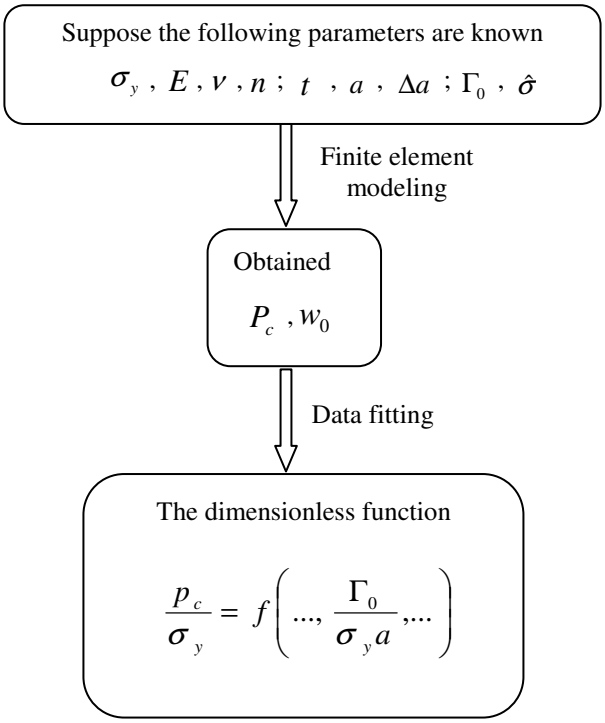
Suppose the following parameters are known
σ_y , E , ν , n ; t , a , Δa ; Γ_0 , $\hat{\sigma}$
Finite element modeling
Obtained
P_c , w_0
Data fitting
The dimensionless function
$\frac{p_c}{\sigma_y} = f\left(..., \frac{\Gamma_0}{\sigma_y a}, ... \right)$

Fig. 2

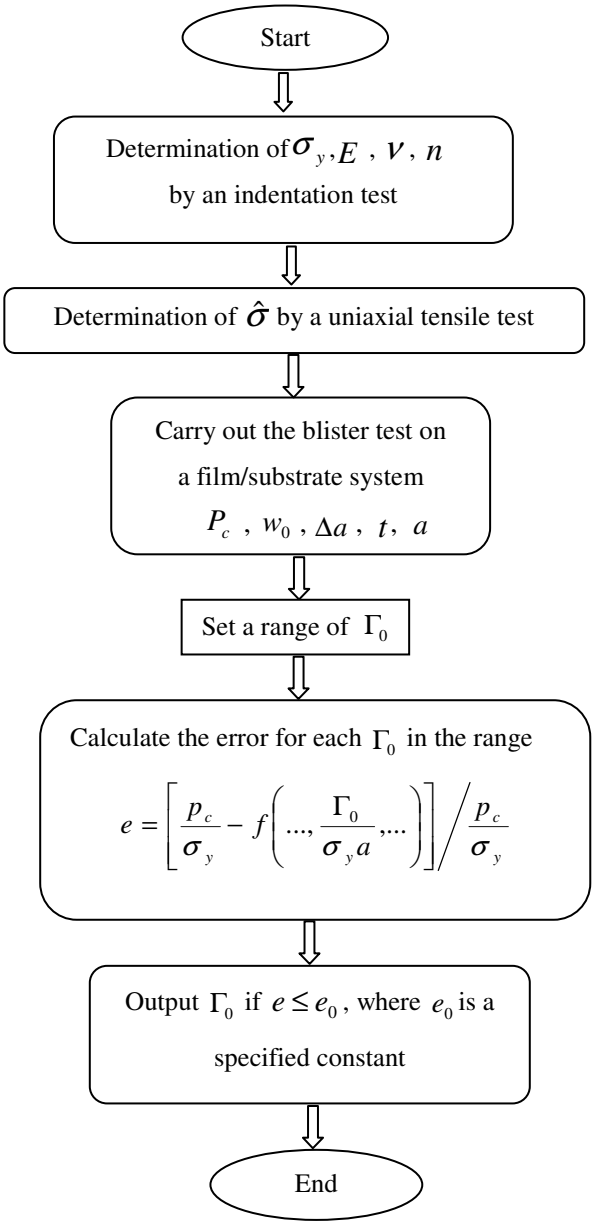
Start
Determination of σ_y, E, ν, n by an indentation test
Determination of $\hat{\sigma}$ by a uniaxial tensile test
Carry out the blister test on a film/substrate system $P_c, w_0, \Delta a, t, a$
Set a range of Γ_0
Calculate the error for each Γ_0 in the range
$e = \left[\frac{p_c}{\sigma_y} - f\left(..., \frac{\Gamma_0}{\sigma_y a}, ... \right) \right] \Big/ \frac{p_c}{\sigma_y}$
Output Γ_0 if $e \le e_0$, where e_0 is a specified constant
End

Fig. 3

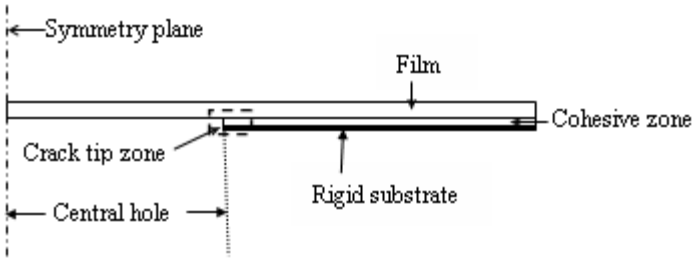
Symmetry plane
Film
Cohesive zone
Crack tip zone
Rigid substrate
Central hole

(a)

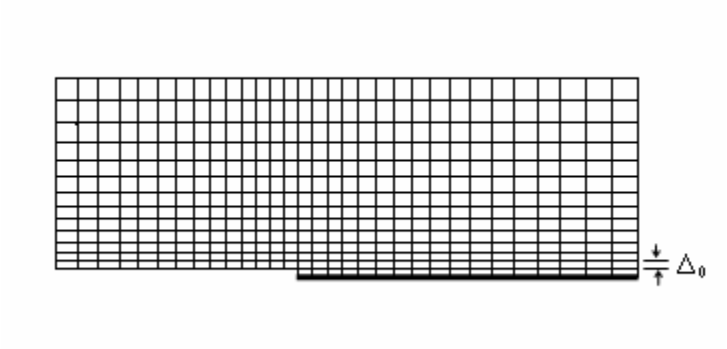
Δ_0

(b)

Fig. 4

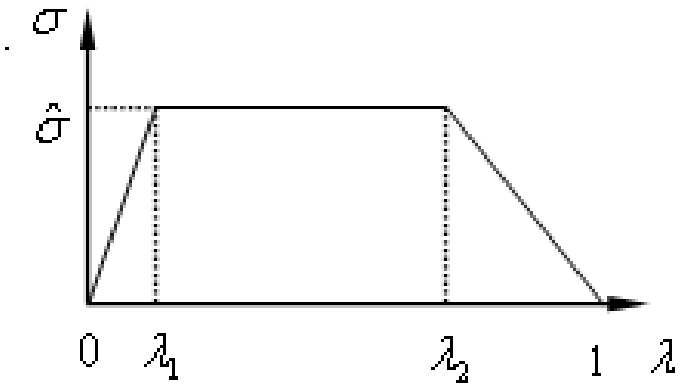

Fig. 5

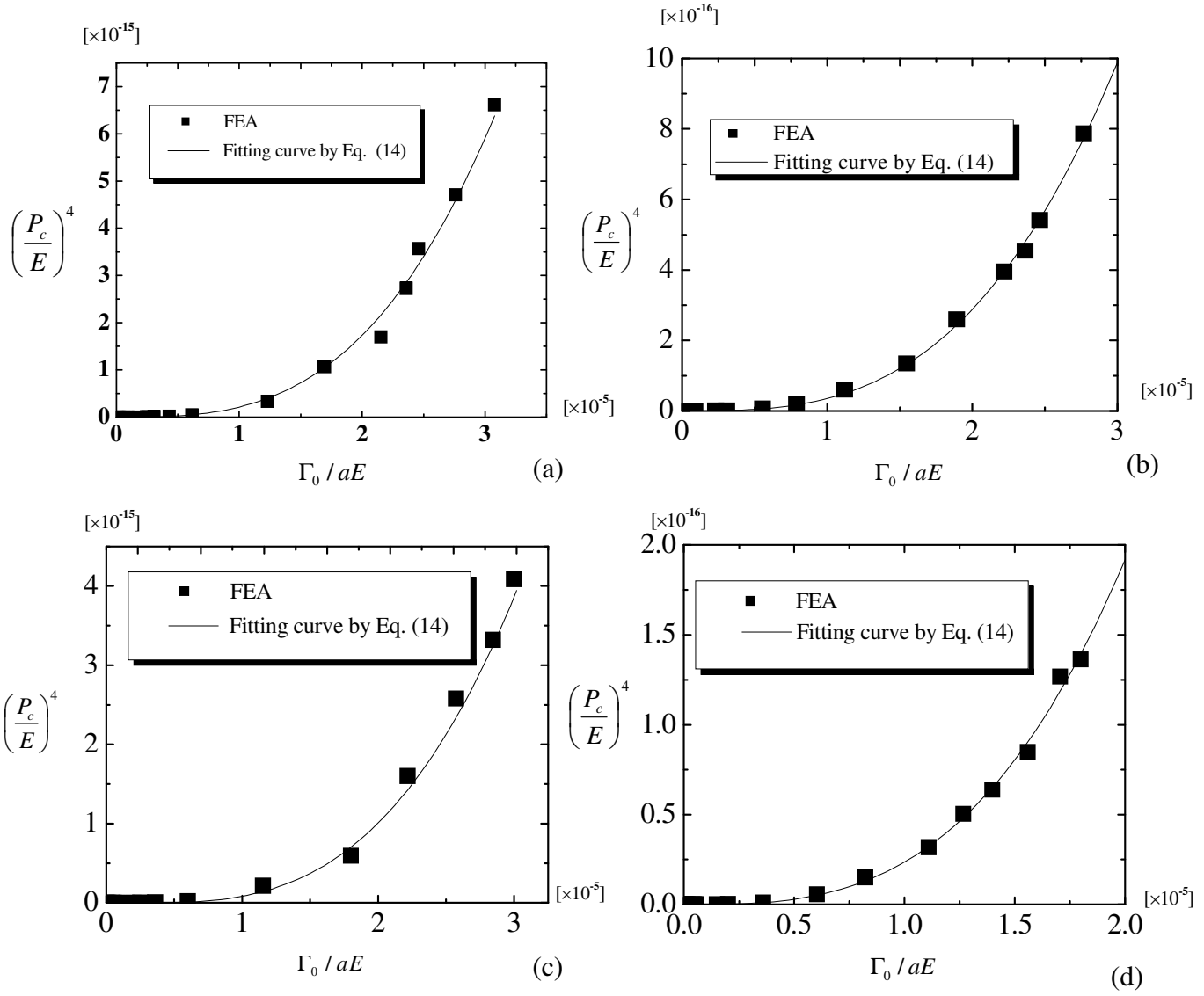
[×10-15]
FEA
Fitting curve by Eq. (14)
$\left(\frac{P_c}{E}\right)^4$
[×10-5]
Γ_0 / aE
(a)
[×10-16]
FEA
Fitting curve by Eq. (14)
$\left(\frac{P_c}{E}\right)^4$
[×10-5]
Γ_0 / aE
(b)
[×10-15]
FEA
Fitting curve by Eq. (14)
$\left(\frac{P_c}{E}\right)^4$
[×10-5]
Γ_0 / aE
(c)
[×10-16]
FEA
Fitting curve by Eq. (14)
$\left(\frac{P_c}{E}\right)^4$
[×10-5]
Γ_0 / aE
(d)

Fig. 6

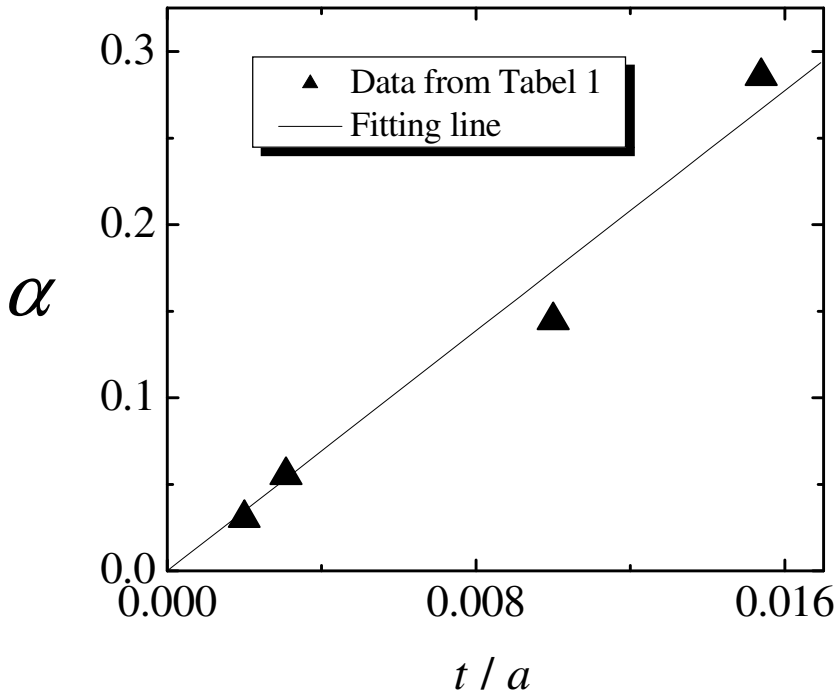

.

Fig. 7

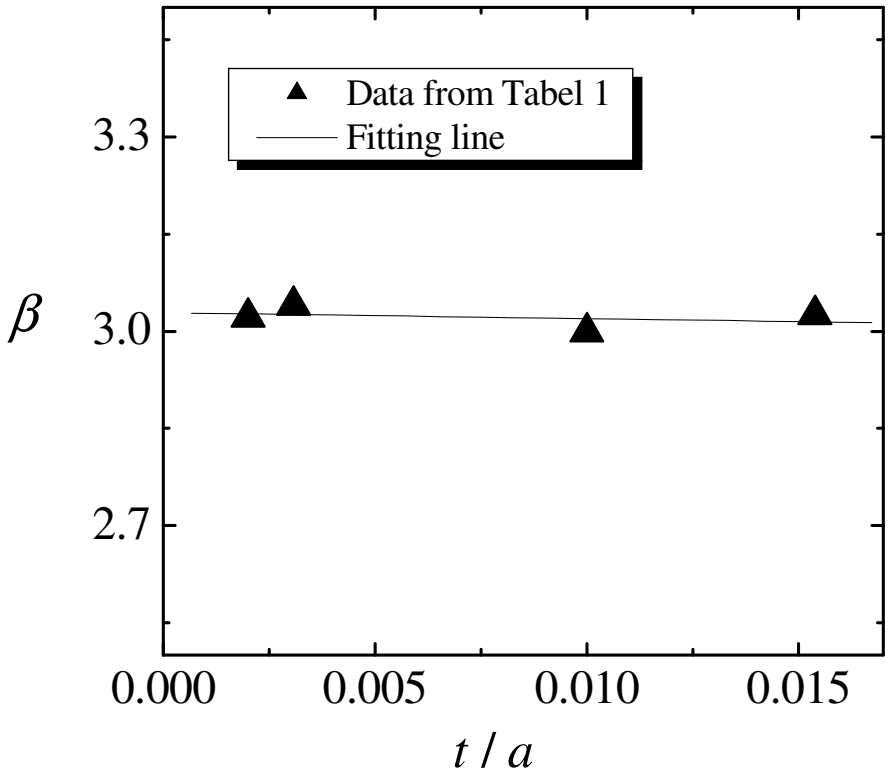
Data from Tabel 1
Fitting line
3.3
3.0
2.7
β
0.000
0.005
0.010
0.015
t / a

Fig. 8

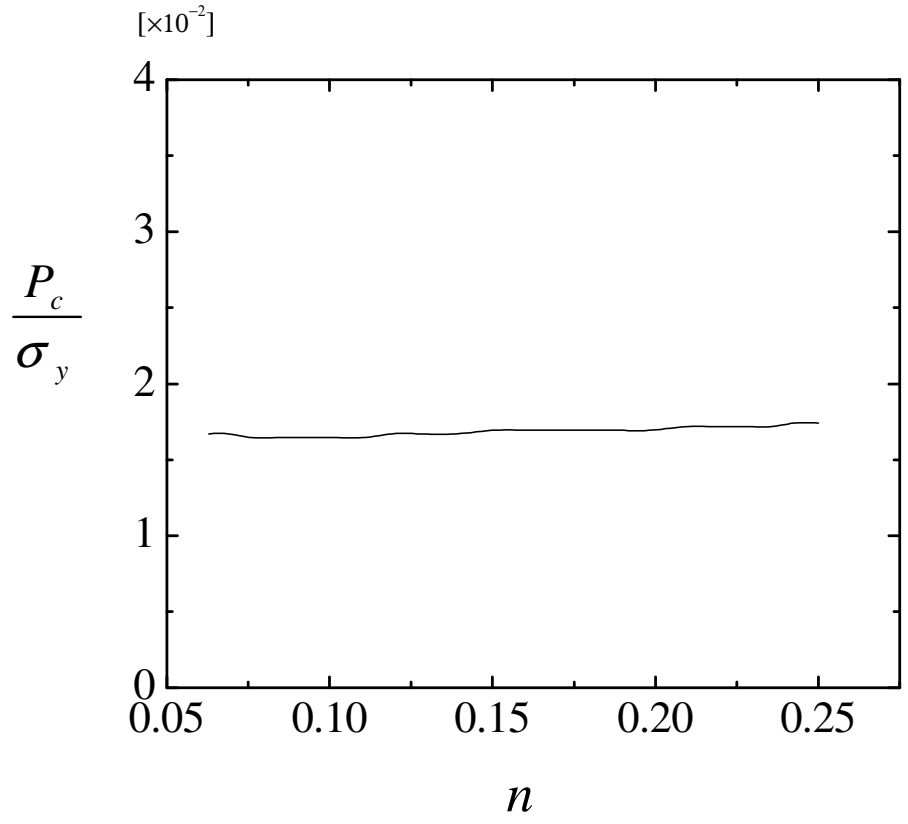

Fig. 9

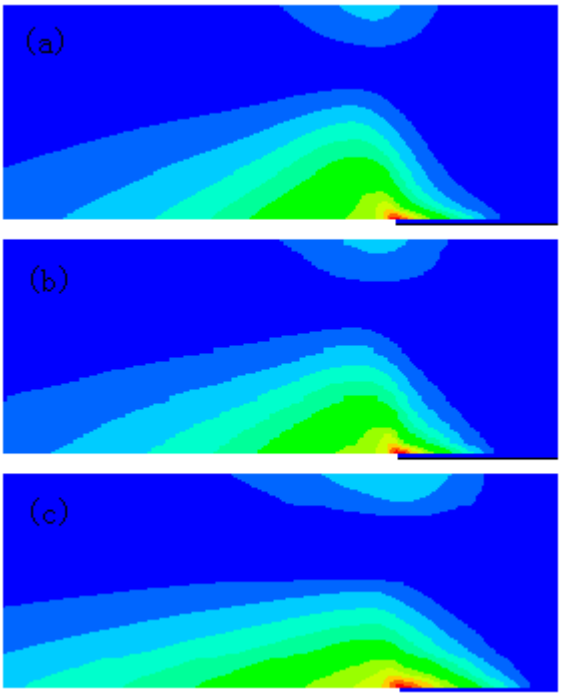

Fig. 10